

The adsorption-controlled growth of LuFe₂O₄ by molecular-beam epitaxy

Charles M. Brooks, Rajiv Misra, Julia A. Mundy, Lei A. Zhang, Brian S. Holinsworth, Kenneth R. O'Neal, Tassilo Heeg, Willi Zander, J. Schubert, Janice L. Musfeldt, Zi-Kui Liu, David A. Muller, Peter Schiffer, and Darrell G. Schlom

Citation: *Applied Physics Letters* **101**, 132907 (2012); doi: 10.1063/1.4755765

View online: <http://dx.doi.org/10.1063/1.4755765>

View Table of Contents: <http://scitation.aip.org/content/aip/journal/apl/101/13?ver=pdfcov>

Published by the AIP Publishing

Articles you may be interested in

[Direct band gaps in multiferroic h-LuFeO₃](#)

Appl. Phys. Lett. **106**, 082902 (2015); 10.1063/1.4908246

[Adsorption-controlled growth of BiVO₄ by molecular-beam epitaxy](#)

APL Mat. **1**, 042112 (2013); 10.1063/1.4824041

[Ferroic investigations in LuFe₂O₄ multiferroic ceramics](#)

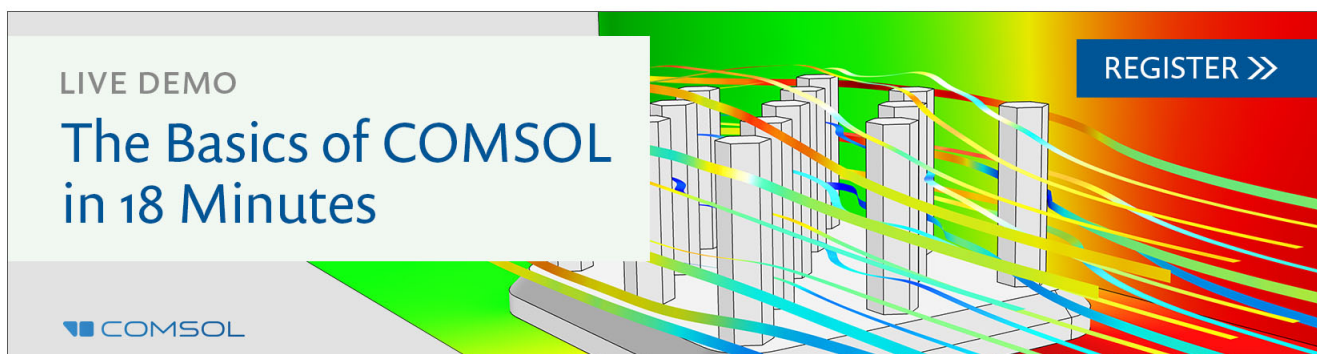
J. Appl. Phys. **110**, 034108 (2011); 10.1063/1.3622147

[Adsorption-controlled growth of BiMnO₃ films by molecular-beam epitaxy](#)

Appl. Phys. Lett. **96**, 262905 (2010); 10.1063/1.3457786

[Adsorption-controlled molecular-beam epitaxial growth of Bi Fe O₃](#)

Appl. Phys. Lett. **91**, 071922 (2007); 10.1063/1.2767771

A promotional banner for a COMSOL live demo. The background features a 3D bar chart with colorful, flowing lines representing data or simulation results. The text 'LIVE DEMO' is in the top left, 'The Basics of COMSOL in 18 Minutes' is in the center, and 'REGISTER >>' is in a blue button in the top right. The COMSOL logo is in the bottom left.

LIVE DEMO

The Basics of COMSOL in 18 Minutes

REGISTER >>

COMSOL

The adsorption-controlled growth of LuFe_2O_4 by molecular-beam epitaxy

Charles M. Brooks,^{1,2} Rajiv Misra,³ Julia A. Mundy,⁴ Lei A. Zhang,² Brian S. Holinsworth,⁵ Kenneth R. O'Neal,⁵ Tassilo Heeg,¹ Willi Zander,⁶ J. Schubert,⁶ Janice L. Musfeldt,⁵ Zi-Kui Liu,² David A. Muller,^{4,7} Peter Schiffer,³ and Darrell G. Schlom^{1,7}

¹*Department of Materials Science and Engineering, Cornell University, Ithaca, New York 14853-1501, USA*

²*Department of Materials Science and Engineering, Pennsylvania State University, University Park, Pennsylvania 16802, USA*

³*Department of Physics and Materials Research Institute, Pennsylvania State University, University Park, Pennsylvania 16802, USA*

⁴*School of Applied and Engineering Physics, Cornell University, Ithaca, New York 14853, USA*

⁵*Department of Chemistry, University of Tennessee, Knoxville, Tennessee 37996, USA*

⁶*Peter Gruenberg Institut (PGI-9), JARA-Fundamentals of Future Information Technologies, Research Centre Jülich, D-52425 Jülich, Germany*

⁷*Kavli Institute at Cornell for Nanoscale Science, Ithaca, New York 14853, USA*

(Received 5 June 2012; accepted 13 September 2012; published online 28 September 2012)

We report the growth of single-phase (0001)-oriented epitaxial films of the purported electronically driven multiferroic, LuFe_2O_4 , on (111) MgAl_2O_4 , (111) MgO , and (0001) 6H-SiC substrates. Film stoichiometry was regulated using an adsorption-controlled growth process by depositing LuFe_2O_4 in an iron-rich environment at pressures and temperatures where excess iron desorbs from the film surface during growth. Scanning transmission electron microscopy reveals reaction-free film-substrate interfaces. The magnetization increases rapidly below 240 K, consistent with the paramagnetic-to-ferrimagnetic phase transition of bulk LuFe_2O_4 . In addition to the ~ 0.35 eV indirect band gap, optical spectroscopy reveals a 3.4 eV direct band gap at the gamma point.

© 2012 American Institute of Physics. [<http://dx.doi.org/10.1063/1.4755765>]

The quest for multiferroics, materials where magnetic order and ferroelectricity coexist, has been challenging due to the frequent incompatibility of the two phenomena.^{1,2} Reports that LuFe_2O_4 is simultaneously ferrimagnetic and ferroelectric below 250 K, the highest temperature of any known material,³ have resulted in significant interest in LuFe_2O_4 . Of late, however, the multiferroic status of LuFe_2O_4 has become controversial.⁴⁻⁷ Unlike more traditional ferroelectrics, LuFe_2O_4 has been reported to develop a ferroelectric polarization from the charge ordering of Fe^{2+} and Fe^{3+} ions.³ This charge ordering mechanism would make LuFe_2O_4 an improper ferroelectric, free of a requisite polar displacement that often precludes the presence of magnetism.² On the other hand, recent experiments have shown that such charge ordering is absent in LuFe_2O_4 ,⁴ that it is not ferroelectric,⁵ and further that the antiferromagnetic order seen in some single crystals⁶ could imply the ferrimagnetic order seen in many samples is due to non-stoichiometry.

The ability to deposit single-crystal thin films of LuFe_2O_4 is a key stepping stone on the path to understanding and manipulating the properties of this material, for example, with strain.^{8,9} There has been some success with growing thin films of LuFe_2O_4 by pulsed-laser deposition (PLD),¹⁰⁻¹² though so far this achievement is limited to polycrystalline films or films with impurity phases present, particularly at the interface. In these cases, the desired LuFe_2O_4 phase only forms with excess iron present during growth by PLD.¹¹ Primary challenges to the growth of higher quality films include the sensitivity of the growth process to substrate temperature and oxygen pressure as well as a lack of suitable substrates.

In this work, we report the deposition of LuFe_2O_4 thin films by molecular-beam epitaxy (MBE) using an adsorption

controlled growth process to control the film composition. The growth method is inspired by that used in the growth of GaAs by MBE.¹³⁻¹⁵ This thermodynamically driven process allows the composition of GaAs to self-limit to the stoichiometric value over a limited growth temperature range despite the substrate being supplied with excess arsenic. A similar process has also been employed as a method of composition-control in MBE-grown oxide thin films of compounds, such as PbTiO_3 and BiFeO_3 .^{16,17} In the case of oxides, oxygen background pressure and substrate temperature are the parameters that define the growth window where stoichiometric film deposition occurs. The growth of LuFe_2O_4 is analogous to that of InFe_2O_4 , which has been achieved in a similar manner at lower temperature using PLD by making use of the volatility of indium at the growth conditions.¹⁸ Here, we use the volatility of iron oxides to achieve phase-pure LuFe_2O_4 by adsorption-controlled growth.

The first step toward achieving epitaxial deposition of LuFe_2O_4 films was uncovering a growth window. The thermodynamic properties of individual phases in the Fe-Lu-O system were developed by means of the CALPHAD method¹⁹ and the phase diagram was calculated using Thermo-Calc²⁰ with a molar ratio of Fe:Lu of 2. These calculations provided the temperature and pressure region where the formation of LuFe_2O_4 is favorable, shown in Fig. 1.

Finding viable substrates providing a suitable template for single-phase epitaxial films of LuFe_2O_4 is also critical. Of commercially available substrates, we identified (111) MgO , (111) MgAl_2O_4 , and (0001) 6H-SiC as candidates for the growth of (0001) LuFe_2O_4 films. The observed epitaxial relationship between (0001) LuFe_2O_4 and the various substrates is shown in Fig. 2(b). The lattice mismatch values for

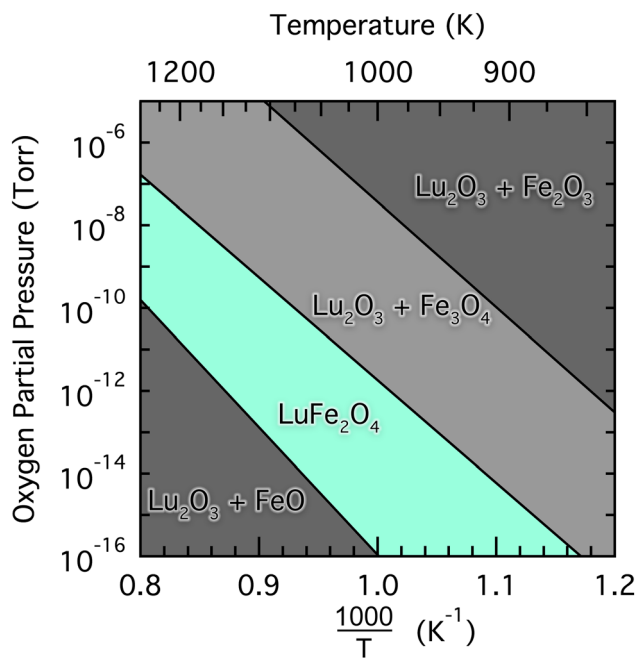


FIG. 1. Arrhenius plot of oxygen partial pressure vs. reciprocal temperature showing where LuFe₂O₄ is thermodynamically stable.

LuFe₂O₄ films on MgO, MgAl₂O₄, and SiC are -15.5% , -4.25% , and -12.0% , respectively.^{21,22}

Using the phase diagram in Fig. 1 as a guide to the adsorption-controlled regime, LuFe₂O₄ films were grown using a Veeco GEN 10 MBE system dedicated to the growth of oxides at a growth temperature of $850 \pm 20^\circ\text{C}$ as measured by optical pyrometry in a background pressure of $\sim 1.0 \times 10^{-6}$ Torr of molecular oxygen. Effusion cells were used to provide elemental fluxes of lutetium and iron. Epitaxial films of LuFe₂O₄ were successfully grown on (111) MgO, (111) MgAl₂O₄, and (0001) 6H-SiC single crystal substrates. Films were typically grown to a thickness of 50 nm and prepared with thicknesses up to 75 nm for optical measurements. In order to ensure the growth of a stoichiometric film, excess iron is required during the deposition process. At a growth temperature of 850°C , much of the supplied iron is evaporated as Fe_xO_y species and is not incorporated into the resulting film. Source fluxes were determined using a quartz crystal microbalance prior to growth. Film structure was monitored periodically throughout the growth by reflection high-energy electron diffraction (RHEED). The lutetium and iron source fluxes were 6.0×10^{12} atoms/(cm² s) and 2.4×10^{13} atoms/(cm² s), respectively, corresponding to an overall lutetium-limited growth rate of ~ 3.2 Å/min. Although the amount of iron supplied is twice that required for the LuFe₂O₄ structure, the excess iron is not incorporated into the film. Rutherford backscattering spectrometry (RBS) was used to verify that the Lu:Fe stoichiometry of the films is indeed 1:2 and that the sticking coefficient of iron is lower at high growth temperatures in the same oxygen background pressure used for the growth of LuFe₂O₄ films.

Four-circle x-ray diffraction (XRD) was performed using a high-resolution Philips X'Pert Pro MRD diffractometer with a PreFix hybrid monochromator on the incident side and triple axis/rocking curve attachment on the diffracted side.

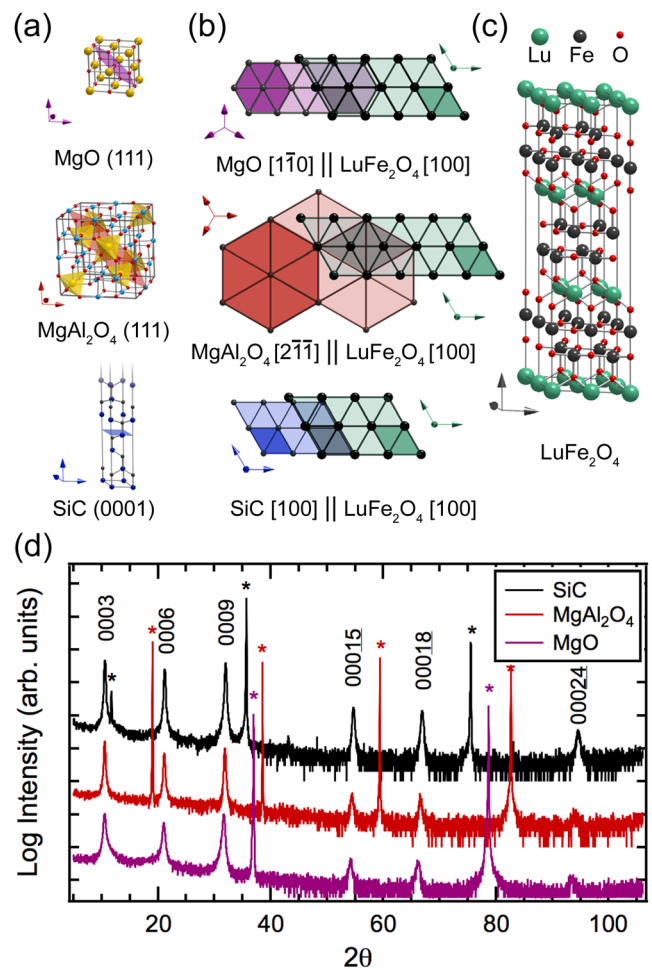


FIG. 2. (a) Substrate model for MgO, MgAl₂O₄, and 6H-SiC with the (111), (111), and (0001) planes of the substrate surface highlighted, respectively. (b) The epitaxial orientation relationship of a LuFe₂O₄ lattice on (111) MgO, (111) MgAl₂O₄, and (0001) 6H-SiC lattices (see Ref. 21). (c) A model showing the alternating single layers of lutetium oxide (U layers, Ref. 24) and double layers of iron oxide (W layers, Ref. 24) in LuFe₂O₄. (d) θ - 2θ x-ray diffraction scans for three 50 nm thick LuFe₂O₄ films grown on (111) MgAl₂O₄, (111) MgO, and (0001) 6H-SiC. Asterisks (*) indicate XRD peaks from the substrates.

Cross-sectional high angle annular dark field scanning transmission electron microscopy (HAADF-STEM) images were recorded on a 100 keV Nion UltraSTEM. The magnetic properties were measured by a Quantum Design superconducting quantum interference device (SQUID) magnetometer in the temperature range from 1.8 to 350 K and magnetic fields up to 70 kOe. RHEED observations provided a convenient indication of proper LuFe₂O₄ phase formation during deposition. Undesired FeO_x phases are readily seen by RHEED in the form of spot patterns while the LuFe₂O₄ phase appears as streaks, indicating a smooth film surface. Since the film oxygen stoichiometry is difficult to quantify, the films may be oxygen deficient, which could affect properties as in the case with YFe₂O₄.²³

The layered LuFe₂O₄ film structure was confirmed by XRD, displayed in Fig. 2, showing that the LuFe₂O₄ films are (0001) oriented and single phase. Despite excess iron being supplied during growth, no iron-rich phases are observed in the films when deposited at 850°C . Some of this excess iron has been observed by RBS to diffuse into the MgAl₂O₄ and MgO substrates. The LuFe₂O₄ film lattice

TABLE I. LuFe₂O₄ film lattice parameters and rocking curve full width at half maximum (FWHM) values determined from XRD data.

Substrate	LuFe ₂ O ₄ film <i>c</i> -axis (Å)	LuFe ₂ O ₄ film <i>a</i> -axis (Å)	Rocking curve FWHM(°)
(111) MgO	25.42 ± 0.01	3.40 ± 0.02	1.13
(111) MgAl ₂ O ₄	25.28 ± 0.01	3.42 ± 0.02	0.76
(0001) 6H-SiC	25.19 ± 0.01	3.44 ± 0.02	0.64

constants and rocking curve results are reported in Table I. The epitaxial orientation relationships between the film and the substrate were verified by ϕ -scans of the 10 $\bar{1}$ 4 LuFe₂O₄ film peak; the [100] LuFe₂O₄ was found to be parallel to [1 $\bar{1}$ 0] MgO, [2 $\bar{1}$ 1] MgAl₂O₄, and [100] 6H-SiC for the substrates studied.

Figure 3 shows STEM images of the interface between the LuFe₂O₄ film and the MgAl₂O₄ substrate viewed down the [100] zone axis of the LuFe₂O₄ film. Notably, the film is

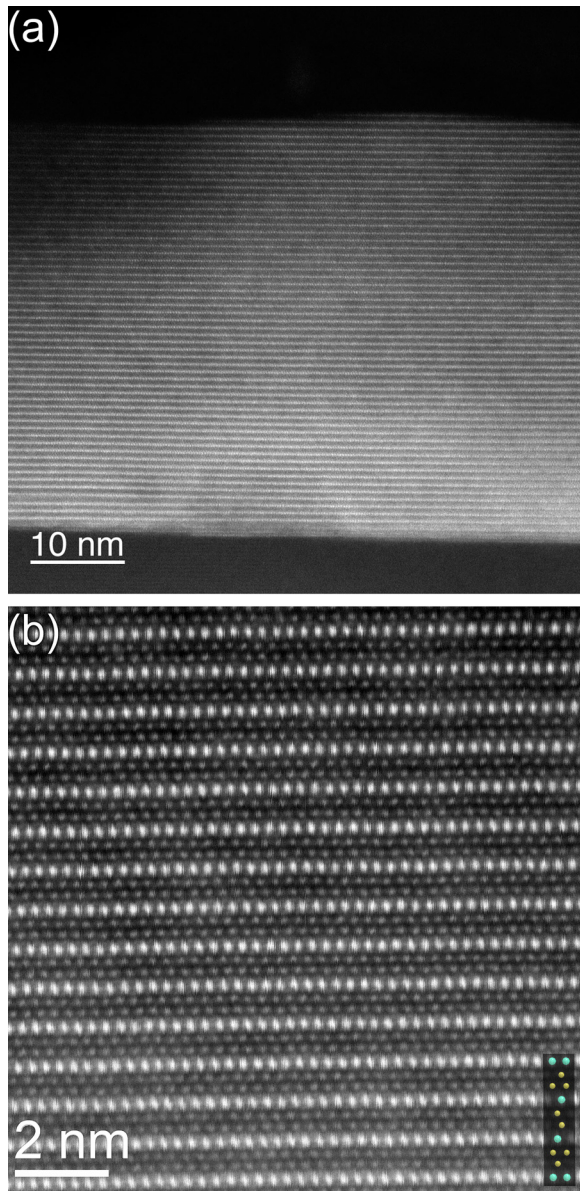


FIG. 3. HAADF-STEM images of the same LuFe₂O₄ on MgAlO₄ film studied in Fig. 2(d) showing (a) the presence of a clean interface and (b) the well-ordered structure of LuO_{1.5} U layers alternating with Fe₂O_{2.5} W layers. An overlay of a single unit cell is shown in the lower corner of (b).

single-phase and free of FeO_x impurity phases at the interface. Figure 3(b) shows a high-resolution image of the film, demonstrating the clear repetition of bright LuO_{1.5} layers (called U layers²⁴) with the darker Fe₂O_{2.5} layers (referred to as W layers²⁴), each of which contains two atomically resolved Fe-O planes.

Magnetization as a function of temperature, displayed in Fig. 4(a), shows that the samples exhibit a singular rapid increase in magnetization below 240 K that is consistent with the bulk paramagnetic to ferrimagnetic phase transition of LuFe₂O₄.²⁵ The samples also display hysteretic behavior with magnetic field, as shown in Fig. 4(b). At 70 kOe, a magnetic moment of about 0.8, 0.3, and 0.1 μ_B per Fe is induced in the films on SiC, MgAl₂O₄, and MgO, respectively. The reduced magnetization in the LuFe₂O₄ film on MgAl₂O₄ and MgO compared to the film on SiC may be due to diffusion of Mg from the substrate into the film since Mg doping has been reported to have this effect.²⁶ The saturation magnetization in our films is lower than the reported bulk value of $\sim 1.4 \mu_B/\text{Fe}$ at 145 kOe.²⁷ While this difference in magnetic moment may be due to the strong dependence on field cooling observed in bulk LuFe₂O₄,²⁷ other factors relating to the deposition process, such as the creation of oxygen vacancies, might be partially responsible. In addition, the samples do not exhibit superparamagnetism, which has been observed in films containing hexagonal LuFeO₃ impurities.¹²

Figure 5 displays the *ab*-plane optical response of LuFe₂O₄ in epitaxial thin film form on MgAl₂O₄ compared with bulk single crystal data.²⁸ Comparison with first

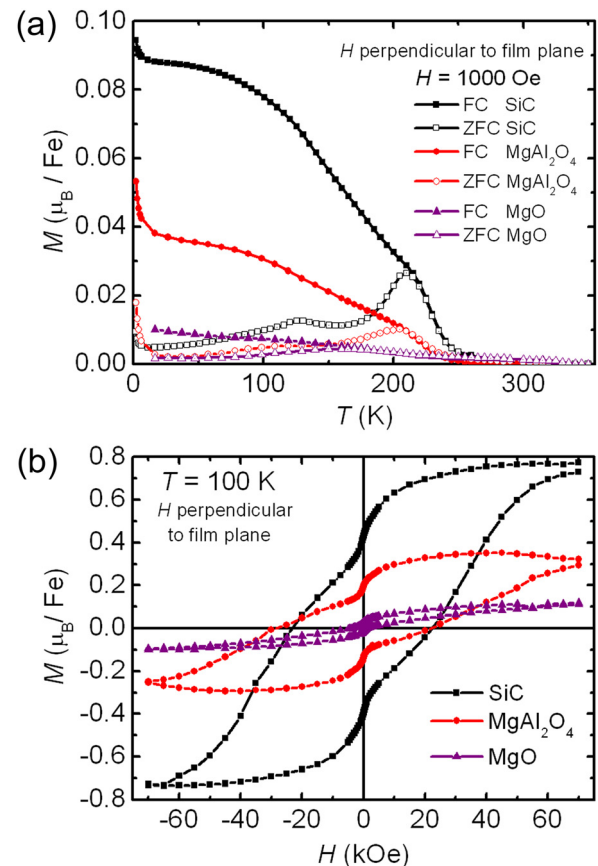


FIG. 4. The magnetization as a function of temperature and magnetic field of the same LuFe₂O₄ films as in Fig. 2(d).

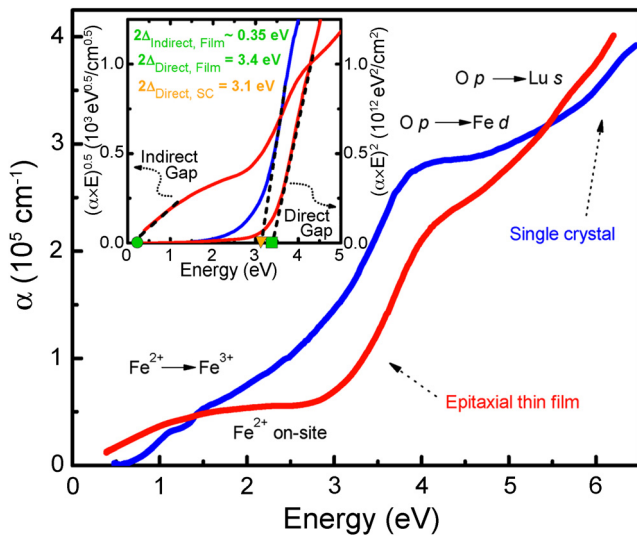


FIG. 5. Optical response of a 75 nm thick (0001) LuFe_2O_4 film grown on (111) MgAl_2O_4 along with the *ab*-plane response of a LuFe_2O_4 single crystal (Ref. 28) at 300 K. The film absorption was determined by a combination of direct calculation of absorption from transmittance (below ~ 3 eV) and a Glover-Tinkham analysis of both transmittance and reflectance to obtain absorption above 3 eV. The data were merged between 2.5 and 3 eV, where there was substantial overlap. The inset shows the indirect and direct band gap analysis.

principles calculations allows us to assign the observed excitations.²⁹ The band centered at ~ 4 eV and the rising higher energy absorption can be assigned as a combination of $O p \rightarrow \text{Fe } d$ and $O p \rightarrow \text{Lu } s$ charge transfer excitations. A plot of $(\alpha \times E)^2$ vs. energy places the direct band gap at ~ 3.4 eV. While the film is not fully commensurate, the average in-plane lattice constant of the film on MgAl_2O_4 from XRD is $3.42 \pm 0.02 \text{ \AA}$, which is 0.6% smaller than the bulk value of 3.44 \AA . This compressive strain blue-shifts the direct charge gap and the band maximum compared to similar structures in the single crystal. BiFeO_3 displays similar behavior.³⁰ Previous measurements on single crystalline LuFe_2O_4 also identified an indirect band gap at ~ 0.35 eV, a feature that is defined by the leading edge of the $\text{Fe}^{2+} \rightarrow \text{Fe}^{3+}$ charge transfer excitations that occur in the W layer (the iron oxide double layer).²⁸ The film shows a similar, but somewhat leakier tendency in the $(\alpha \times E)^{0.5}$ vs. energy plot, although due to limited optical density, our uncertainties are larger. Similar measurements on a film on SiC are less interpretable due to the 3.05 eV band gap of the substrate.

In summary, we have identified a reliable method for depositing single-phase epitaxial LuFe_2O_4 films. This ability combined with the knowledge that the charge-order transition temperature of LuFe_2O_4 is sensitive to pressure³¹ invites the use of thin film methods, e.g., strain or dimensional confinement through heterostructuring, to modify the structure and properties of this controversial multiferroic.

Research supported by the U.S. Department of Energy, Office of Basic Energy Sciences, Division of Materials Sciences, and Engineering under Award Nos. DE-SC0002334 (sample synthesis and characterization) and DE-FG02-01ER45885 (spectroscopy). C.M.B. acknowledges stipend support from the National Science Foundation through the MRSEC program (DMR-0820404). J.A.M. acknowledges

financial support from a National Defense Science & Engineering Graduate Fellowship. Electron microscopy facility support through the NSF MRSEC program (DMR 1120296) and NSF IMR-0417392. We thank P. Chen for useful discussions.

- ¹N. A. Hill, *J. Phys. Chem. B* **104**, 6694–6709 (2000).
- ²S.-W. Cheong and M. Mostovoy, *Nature Mater.* **6**, 13–20 (2007).
- ³N. Ikeda, H. Ohsumi, K. Ohwada, K. Ishii, T. Inami, K. Kakurai, Y. Murakami, K. Yoshii, S. Mori, Y. Horibe, and H. Kito, *Nature* **436**, 1136–1138 (2005).
- ⁴J. de Groot, T. Mueller, R. A. Rosenberg, D. J. Keavney, Z. Islam, J.-W. Kim, and M. Angst, *Phys. Rev. Lett.* **108**, 187601 (2012).
- ⁵A. Ruff, S. Krohns, F. Schrettle, V. Tsurkan, P. Lunkenheimer, and A. Loidl, *Eur. Phys. J. B* **85**, 290 (2012).
- ⁶J. de Groot, K. Marty, M. D. Lumsden, A. D. Christianson, S. E. Nagler, S. Adiga, W. J. H. Borghols, K. Schmalz, Z. Yamani, S. R. Bland, R. de Souza, U. Staub, W. Schweika, Y. Su, and M. Angst, *Phys. Rev. Lett.* **108**, 037206 (2012).
- ⁷X. S. Xu, J. de Groot, Q.-C. Sun, B. C. Sales, D. Mandrus, M. Angst, A. P. Litvinchuk, and J. L. Musfeldt, *Phys. Rev. B* **82**, 014304 (2010).
- ⁸J. H. Haeni, P. Irvin, W. Chang, R. Uecker, P. Reiche, Y. L. Li, S. Choudhury, W. Tian, M. E. Hawley, B. Craigo, A. K. Tagantsev, X. Q. Pan, S. K. Streiffer, L. Q. Chen, S. W. Kirchoefer, J. Levy, and D. G. Schlom, *Nature* **430**, 758–761 (2004).
- ⁹K. J. Choi, M. Biegalski, Y. L. Li, A. Sharan, J. Schubert, R. Uecker, P. Reiche, Y. B. Chen, X. Q. Pan, V. Gopalan, L.-Q. Chen, D. G. Schlom, and C. B. Eom, *Science* **306**, 1005–1009 (2004).
- ¹⁰R. Rejman, T. Dhakal, P. Mukherjee, S. Hariharan, and S. Witanachchi, in *Multiferroic and Ferroelectric Materials*, edited by A. Gruverman, C. J. Fennie, I. Kunishima, B. Noheda, and T. W. Noh, (Mater. Res. Soc. Symp. Proc., 2010), Vol. 1199, p. F03–22.
- ¹¹J. Liu, Y. Wang, and J. Y. Dai, *Thin Solid Films* **518**, 6909–6914 (2010).
- ¹²W. Wang, Z. Gai, M. Chi, J. D. Fowlkes, J. Yi, L. Zhu, X. Cheng, D. J. Keavney, P. C. Snijders, T. Z. Ward, J. Shen, and X. Xu, *Phys. Rev. B* **85**, 155411 (2012).
- ¹³J. R. Arthur, *J. Appl. Phys.* **39**, 4032 (1968).
- ¹⁴A. Y. Cho, *J. Appl. Phys.* **41**, 2780 (1970).
- ¹⁵A. Y. Cho, *J. Appl. Phys.* **42**, 2074 (1971).
- ¹⁶C. Theis and D. G. Schlom, *Thin Solid Films* **325**, 107–114 (1998).
- ¹⁷J. F. Ihlefeld, A. Kumar, V. Gopalan, D. G. Schlom, Y. B. Chen, X. Q. Pan, T. Heeg, J. Schubert, X. Ke, P. Schiffer, J. Orenstein, L. W. Martin, Y. H. Chu, and R. Ramesh, *Appl. Phys. Lett.* **91**, 071922 (2007).
- ¹⁸M. Seki, T. Konya, K. Inaba, and H. Tabata, *Appl. Phys. Express* **3**, 105801 (2010).
- ¹⁹Z. K. Liu, *J. Phase Equilib. Diffus.* **30**, 517–534 (2009).
- ²⁰J. O. Andersson, T. Helander, L. Hoglund, P. Shi, and B. Sundman, *CALPHAD: Comput. Coupling Phase Diagrams Thermochem.* **26**, 273–312 (2002).
- ²¹These mismatch values correspond to the observed epitaxial orientation relationship for these systems (described in Fig. 2), where we have assumed near-coincident site lattices (NCSL) with σ -boundary ratios at the interfaces of $\sigma_{\text{MgO}} 1 : \sigma_{\text{LuFe}_2\text{O}_4} 1$, $\sigma_{\text{MgAl}_2\text{O}_4} 1 : \sigma_{\text{LuFe}_2\text{O}_4} 3$, and $\sigma_{\text{SiC}} 1 : \sigma_{\text{LuFe}_2\text{O}_4} 1$. The areas of the NCSL unit cells for these cases are 0.077 nm^2 , 0.283 nm^2 , and 0.081 nm^2 , respectively. For additional information on NCSL, see Ref. 22.
- ²²R. W. Balluffi, A. Brokman, and A. H. King, *Acta Metall.* **30**, 1453–1470 (1982).
- ²³M. Inazumi, Y. Nakagawa, M. Tanaka, N. Kimizuka, and K. Siratori, *J. Phys. Soc. Jpn.* **50**, 438–444 (1981).
- ²⁴T. Sugihara, K. Siratori, N. Kimizuka, J. Iida, H. Hiroyoshi, and Y. Nakagawa, *J. Phys. Soc. Jpn.* **54**, 1139–1145 (1985).
- ²⁵J. Wen, G. Xu, G. Gu, and S. M. Shapiro, *Phys. Rev. B* **80**, 020403(R) (2009).
- ²⁶Y. B. Qin, H. X. Yang, Y. Zhang, H. F. Tian, C. Ma, Y. G. Zhao, R. I. Walton, and J. Q. Li, *J. Phys.: Condens. Matter* **21**, 015401 (2009).
- ²⁷J. Iida, M. Tanaka, Y. Nakagawa, S. Funahashi, N. Kimizuka, and S. Takekawa, *J. Phys. Soc. Jpn.* **62**, 1723–1735 (1993).
- ²⁸X. S. Xu, M. Angst, T. V. Brinzari, R. P. Herman, J. L. Musfeldt, A. D. Christianson, D. Mandrus, B. C. Sales, S. McGill, J.-W. Kim, and Z. Islam, *Phys. Rev. Lett.* **101**, 227602 (2008).
- ²⁹H. J. Xiang and M.-H. Whangbo, *Phys. Rev. Lett.* **98**, 246403 (2007).
- ³⁰P. Chen, N. J. Podraza, X. S. Xu, A. Melville, E. Vlahos, V. Gopalan, R. Ramesh, D. G. Schlom, and J. L. Musfeldt, *Appl. Phys. Lett.* **96**, 131907 (2010).
- ³¹X. Shen, C. H. Xu, C. H. Li, Y. Zhang, Q. Zhao, H. X. Yang, Y. Sun, J. Q. Li, C. Q. Jin, and R. C. Yu, *Appl. Phys. Lett.* **96**, 102909 (2010).